 MCB, vol.15, no.1, pp.51-61, 2018

Study on the Contact Stress Concentration and the Hyperplasia of the Canine Trachea Granulation Tissue after Stenting

Zhiguo Zhang[1, *], Ming Zhu[1, 2], Xiaowei Yu[3], Xiaohao Shi[1], Chen Jiang[1, 2], Yimin Sun[1, 2], Ming Zhang[4], Yue Wang[1], Yuqiao Wen[5] and Chingcheng Huang[6]

Abstract: Tracheal stenosis is a common respiratory disease and is usually treated by stent implantation. However, the implanted stent often causes excessive hyperplasia of trachea granulation tissue, leading to the restenosis. Although surgical removal or chemical suppression can be used to alleviate the restenosis, the efficacy is limited. Thus, restenosis remains a thorny complication. We investigated this issue from the perspective of the "stress-growth" relationship. Firstly, the lower airway of 5 experimental dogs were CT-scanned to reconstruct the 3D numerical models; secondly, the implantations of the Nitinol alloy stents were numerically simulated; thirdly, 45 days after the stenting, the dogs were evaluated for the hyperplasia of the trachea granulation tissue by CT imaging, bronchoscopy and histological sectioning; finally, the correlation analysis was performed between the contact stress and the hyperplasic thickness of the granulation tissue. Results show that the hyperplasia of the trachea granulation tissue and the local contact stress are positively correlated (R=0.82) and the high local dilation stress can promote the hyperplasia of the trachea granulation tissue, probably through the recombination of basic fibroblast growth factor or the dysfunction of plasminogen activator inhibitor-1. Therefore, contact stress concentration should be prevented in the future design of the tracheal stent.

Keywords: Tracheal restenosis, trachea granulation tissue, contact stress concentration, "Stress-growth" relationship, 3D numerical model.

[1] Institute of Biomedical Engineering and Health Sciences, Changzhou University, Changzhou, Jiangsu, China.

[2] School of Mechanical Engineering, Changzhou University, Changzhou, Jiangsu, China.

[3] Department of Respiration, Changzhou No.2 People's Hospital, Changzhou, Jiangsu, China.

[4] Thoracic and Cardiovascular Surgery, Changzhou No.2 People's Hospital, Changzhou, 213003, China.

[5] School of Automation and Electronic Information, Sichuan University of Science & Engineering, Zigong, 643000, China.

[6] Department of Biomedical Engineering, Mingchuan University, Taoyuan, 111, China.

* Corresponding author: Zhiguo Zhang. Email: 1930534@qq.com.

1 Introduction

Tracheal stenosis is a pathological condition that the airway lumen is narrowed due to various reasons, which impairs lung ventilation and thus can cause severe dyspnea or even suffocation if not treated timely and effectively [Kampmann, Wiethoff, Huth et al. (2017)]. Clinically, the most effective treatment for tracheal stenosis is stenting, which immediately expands the narrowed airway and relieves the breath difficulty of the patient, showing significant short-term efficacy [Nashef, Dromer, Velly et al. (1992); Shaikh, Kichenadasse, Choudhury et al. (2013)]. A typical type of airway stent is made of metallic Nitinol memory wires, which is still widely used in developing countries such as China because of its low cost. Such stents can easily be implanted through a flexible bronchoscope, and provides good radial support and epithelialization, thereby reducing the risk of migration and obstruction by mucus [Chaure, Serrano, Fernández-Parra (2016)]. However, implantation of the Nitinol alloy stent (NAS) is often accompanied by many complications, such as acute inflammation, airway wall fibrosis and hyperplasia of trachea granulation tissue (HTGT) or sometimes sarcoma tissue through the stent holes that leads to restenosis [Fernandez-Bussy, Akindipe, Kulkarni et al. (2009); Xu, Xu, Zhang et al. (2016)]. HTGT occurs in more that 50% of the patients who received stent implantation [Grewe, Müller, Lindstaedt et al. (2005)], especially in those susceptible to infections or scars [Matt, Myer, Harrison et al. (1991); Xu, Ma, Wu et al. (2016)] making it the most problematic complication associated with metal stent implantation.

Although laser surgery together with budesonide treatment and coated/drug-loaded stents are available to be used for ablation or suppression of the hyperplasia of granulation tissue following stent implantation, the efficacy of such therapeutic interventions in preventing in vivo granulation is so far very limited [Gesierich, Reichenberger, Fertl et al. (2014); Yokoi, Nakao, Bitoh et al. (2014)]. The reason is largely because we do not fully understand the mechanism of the granulation. Previous studies on the excessive tissue growth have mainly focused the role of immune and/or inflammatory responses. For example, Ghosh et al. [Ghosh, Malaisrie, Leahy et al. (2011)] demonstrated that formation of granulation tissue is largely regulated by circulating B cells and T cells. Pokharel et al. [Pokharel, Maeda, Yamamoto et al. (1999)] found a large number of capillaries in the granulation tissue with increased permeability, number of fibroblasts, and expression of growth factors including tranfroming growth factor (TGF) and vascular endothelial growth factor (VEGF)-β1. When fibroblasts and these growth factors (TGF and VEGF) are inhibited or targeted in the granulation tissue, HTGT can be reduced [Lee, Hung, Liu et al. (2011)].

Comparing to those widely studied biochemical factors, biomechanical factors have hardly been considered in causing HTGT, despite that “stress-growth” relationship is generally regarded as the universal biomechanical principle in determining tissue growth at all levels of the human body (organ, tissue, cell, subcellular structure, biological macromolecules and polymers). In fact, it is well known that mechanical environment (stress field) largely affects the structure and function including growth of the tissue and cell [Fung (1995); Zöllner, Abilez, Böl et al. (2012)]. Therefore, we speculated that the excessive HTGT subsequent to implantation of the airway stent into trachea may well be related to the change of local mechanical environment due to the presence of the stent.

Thus, this study aimed to investigate the effect of the NAS implantation on both stress distributions in the tracheal wall by numerical simulation, and the hyperplasia of the trachea granulation tissue (HTGT) by experimental observation in dogs. Such biomechanical perspective may be helpful to improve the design of airway stents to better reduce the incidence of trcheal restenosis after stenting.

2 Materials and methods

2.1 Contact stress analysis of NAS implantation

2.1.1 Numerical model of trachea

Thoracic CT scans were taken from 5 experimental dogs. About 1300 images were obtained for each dog (DICOM format, 512×512 arrays, pitch 0.3 mm). Then, they were imported into Mimics 9.0 and post-processed to reconstruct the 3D numerical models of the trachea. Finally, to ensure the quality of the finite element meshes, the trachea models were imported into 3-Matic STL 9.0 for repeated triangle reduction and surface smoothing, as shown in Fig. 1.

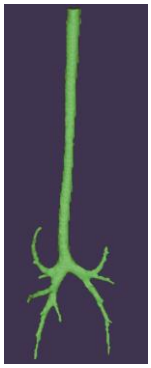

Figure 1: The reconstructed 3D trachea numerical model

The tracheal wall was assumed to be incompressible, isotropic hyperelastic material and meshed with 35786 3D solid elements. Its mechanical behavior was described in terms of engineering strain and piecewise spline interpolations of uniaxial tension-compression test data, as shown in Fig. 2 [Sussman and Bathe (2009)].

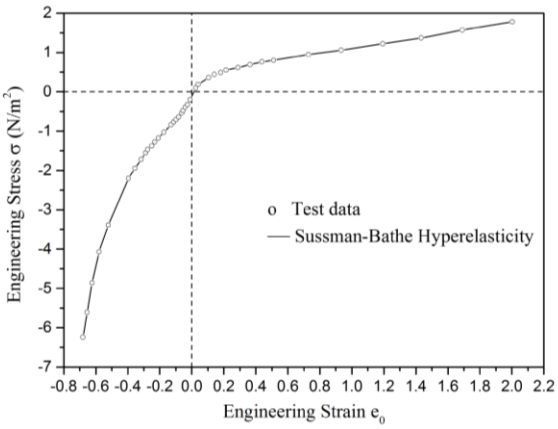

Figure 2: The "stress-strain" curve of the trachea wall

2.1.2 Numerical model of NAS

In order to reduce the risk of slippage, the site 150 mm above carina was chosen as the center of implanted NAS. Then the trachea diameters above and below the center (±20 mm) were measured based on the CT images imported into Mimics 9.0. The calculated average diameter of the selected trachea was about 11.6 mm. According to clinical experience, the diameter of the stent should be at least 20% larger than the trachea. Hence, the diameter of the implanted NAS (Changzhou Zhiye Medical Devices Institute Co., Ltd., Changzhou, Jiangsu, China) was set to 14 mm with the length of 40 mm. The 3D numerical model reconstruction of the NAS was performed with ADINA9.0. The stent was defined as a beam element (1056 Hermitian beam elements) with a circular cross section. The detailed geometrical and mechanical parameters are listed in Tab. 1. Fig. 3(A) shows the numerical model of the NAS, the green dots indicate intersections of the guidewire (hinge point).

Table 1: Parameters used to define the geometry and mechanical properties of the NAS

Stent Diameter (mm)	Stent Length (mm)	Guidewire Diameter (mm)	E (KPa)	ν
14	40	0.23	40×10^6	0.33

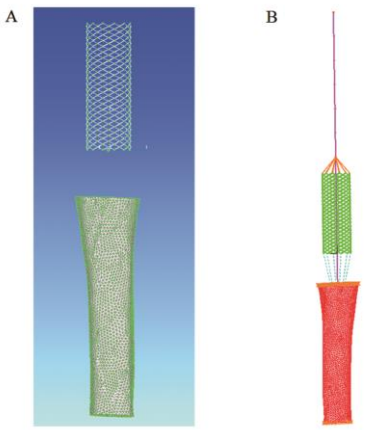

Figure 3: (A) Alignment of the stent with the tracheal wall; (B) Establishment of auxiliary instrument of the stent

2.1.3 Contact stress analysis

First, the stent was aligned with the tracheal wall in the FEMAP software, as shown in Fig. 3 (A). Then, the models were imported into ADINA9.0 to establish auxiliary instrument of the stent, as shown in Fig. 3 (B). Finally, radially expanding displacement load (10% of the averaged trachea diameter) was applied to the stent in ADINA9.0, meanwhile, interaction between the stent and the tracheal wall was simulated using implicit constraint function method, and the constraint function for frictional contact as shown in Eq. (1):

$$w(g,\lambda) = \frac{g+\lambda}{2} - \sqrt{\left(\frac{g-f}{2}\right)^2 + \varepsilon_N} \quad (1)$$

wherein, g is a gap between contact surfaces, λ is the normal contact force, f is the normalized friction variable and ε_N is a user-defined parameter, whose default value is 10^{-12}. During the process of simulation, only the radial and axial displacements were allowed, any rotation was forbidden. The top of the trachea was fixed.

Fig. 4 shows the top view of the stent implantation process, it can be observed that the stent was first stretched into a thinner shape and put into the lower airway, then upon reaching the predetermined position, and then the stent began to expand to its original diameter.

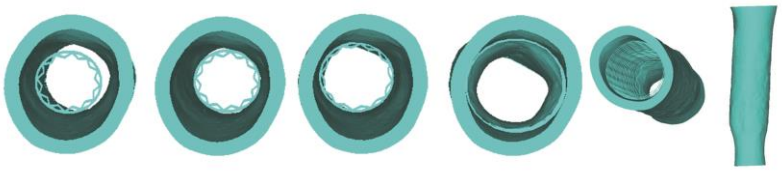

Figure 4: Top and front view of the stent implantation process

2.2 Animal experiments of HTGT after NAS implantation

Animal experiments were performed with the assistance from Changzhou Second People's Hospital, and the whole process is strictly in line with the national animal experiments regulations. The procedures are as follows: 5 adult mongrel dogs weighing 13-17 kg were selected for experiment, irrespective of gender. The dogs were closely monitored since 3 days before surgery, and all 5 dogs showed normal diet and breathing. Before implantation, the dogs were anesthetized by intraperitoneal injection of pentobarbital sodium. Then, they were fixed in supine position on the operating table for airway stenting. It was required the stent being positioned at 150 mm above the carina. To quantitatively study the hyperplasia of granulation tissue, chest of the dogs was examined by CT scan again after 45 days and the CT data were imported into Mimics to observe the hyperplasia from different angles. In the meantime, the fiber bronchoscopy and biopsy were performed.

3 Results

3.1 Distribution of contact stress between the NAS and the tracheal wall

Fig. 5 shows the stress distribution inside (A) and outside (B) of the airway. It can be observed that the stress was not evenly distributed on the airway wall, but concentrated at some areas, especially in the lower part of the stented area, where the largest stress to the airway wall was up to 1.56 Mpa.

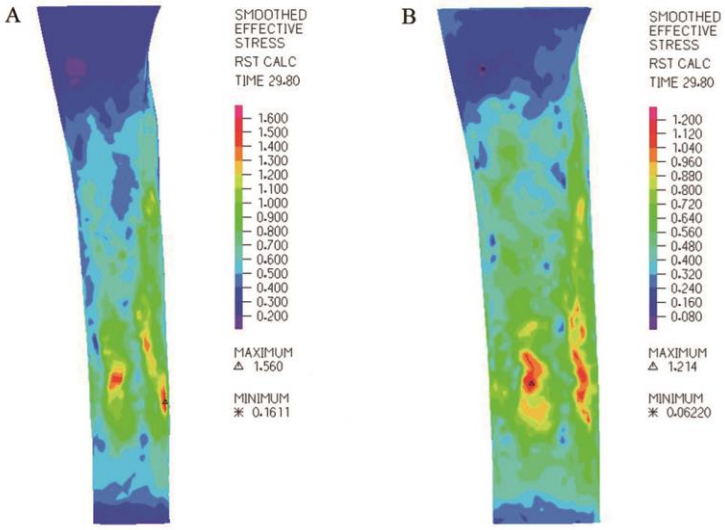

Figure 5: Stress distribution inside and outside of the airway: (A) inner side; (B) outer side

3.2 Hyperplasia of tracheal granulation tissue in experimental dogs after stenting

After 45 days of stenting, HTGT was quantitatively assessed by CT, bronchoscopy, and histological sectioning. Bronchoscopy (PENTAX EB-1530T3, Japan) and supporting

camera device revealed significant hyperplasia of granulation tissue, and the hyperplasia was more severe at the lower part of the stented airway, as shown in Fig. 6 (A). Fig. 6 (B) demonstrates the microstructure of the tracheal wall tissue at 40X magnification, in which we can see clearly large number of capillaries and squamous metaplasia, suggesting that granulation is the major reason of tracheal stenosis.

Arrows in Fig. 6 (C) and (D) indicates constriction of the airway, the white dots indicate the high-density NAS, and the gray area within the frame of the stent represents hyperplastic granulation tissue that grows through the stent mesh. As shown in the figure, hyperplasia mainly occurs at the lower part of the stented airway, and stenosis was up to 90% at the most occluded area, this result is in line with what's found by bronchoscopy. Meanwhile, contact stress analysis showed severe stress concentration at these sites.

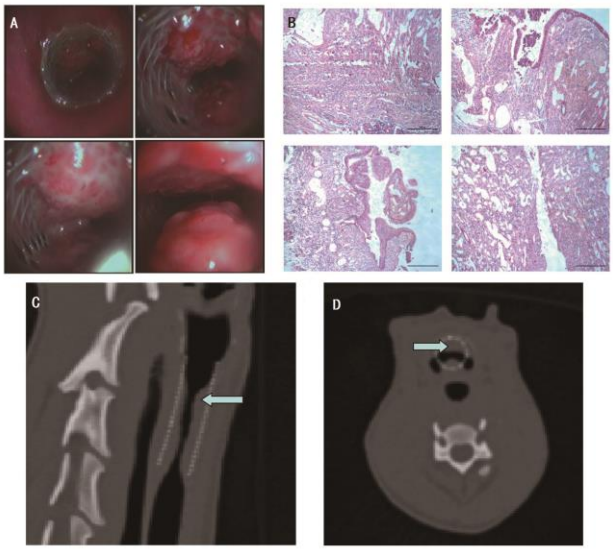

Figure 6: (A) Bronchoscopy results; (B) Histological sections of the narrowed tracheal wall; (C) Sagittal view of the observed granulation tissue growth; (D) Axial view of the hyperplastic granulation tissue

3.3 Correlation between contact stress concentration and HTGT

To further clarify the correlation between hyperplasia of granulation tissue and local mechanical environment, 10 highly stressed areas, A_1-A_{10} were selected from the stress distribution map for each dog (Fig. 7 (L)). The max averaged stress of each area (δ_{max}) and the max thickness of the hyperplastic granulation tissue (H_{max}) were calculated and measured for each dog. The averaged valuves of δ_{max} and H_{max} for the 5 adopted dogs were shown in Fig. 7 (R). Correlation analysis suggestes that HTGT is positively correlated with the value of local stress, with a correlation coefficient of 0.82 (p<0.05, Fig. 8). The larger stress, the more severe hyperplasia (A_9 showed the most severe hyperplasia of granulation tissue and suffered the largest average stress).

The purpose of the present study was to investigate the excessive hyperplasia of tracheal granulation tissue caused by the Nitinol alloy stent implantation, from the biomechanical perspective of "stress-growth" relationship. Our results show that HTGT and local contact stress are positively correlated, indicating that stress concentration can promote the hyperplasia of tracheal granulation tissue. It has been known that proto-myofibroblasts begin moving from the unaffected tissue toward the wound center after stenting and evolve generally into α-SM actin containing differentiated myofibroblasts [Tomasek, Gabbiani, Hinz et al. (2002)]. Normally, myofibroblasts will vanish through apoptosis and a scar will persist in the affected area after the wound healing [Desmoulière, Redard, Darby et al. (1995)]. However, in present study, myofibroblasts persisted in a closed wound and resulted in a hypertrophic scar after the trachea stent implantation [Tomasek, Gabbiani, Hinz et al. (2002); Van De Water, Varney and Tomasek (2013)]. The possible reason for it is that the recombinant basic fibroblast growth factor (rbFGF) casued by the local high dilation stress may lead to the possible loss of the normal signals required to stop repair, hence result in a marked delay in wound healing [Pierce, Tarpley, Yanagihara et al. (1992)]. Another possible reason for it is that the dysfunction of plasminogen activator inhibitor-1 (PAI-1) casued by the local high dilation stress. PAI-1 is a key regulator of the tissue repair program and impacts cellular responses to tissue injury and stress situations (growth, survival and migration) [Simone and Higgins (2015)].

L

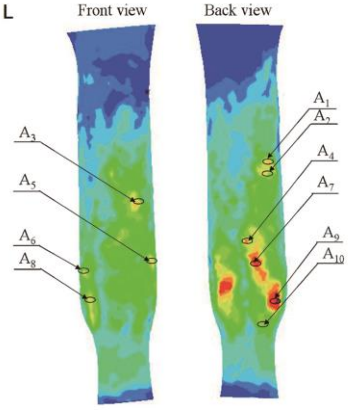

R

A_n	δ_{max} (MPa)	H_{max} (mm)
A_1	1.23	5.74
A_2	1.22	6.08
A_3	1.25	6.25
A_4	1.33	6.08
A_5	1.29	6.32
A_6	1.03	4.9
A_7	1.47	6.59
A_8	1.21	5.57
A_9	1.56	6.92
A_{10}	1.30	6.36

Figure 7: (L) The highly stressed areas on the inner airway wall (A_1-A_{10}); (R) The averaged δmax and Hmax for the 5 adopted dogs

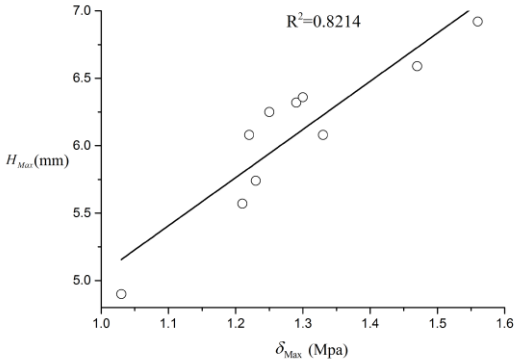

Figure 8: Correlation analysis between the max averaged stress (δmax) and the max hyperplastic thickness of the granulation tissue (Hmax) of the 5 adopted dogs (n=5, $p<0.05$)

4 Discussion

In conclusion, the current NAS used in clinical practice are basically in unified geometry and size, irrespective of the variations in airway shape and size among different patients. Such NAS is bound to cause stress concentration and prone to slippage after implantation. Therefore, stress concentration should be prevented in the design of NAS. The results of this study show a promise for the inhibition of HTGT through design and manufacture of patient-specific NAS according to each patient's trachea anatomy, and use of appropriate biocompatible materials and rapid prototyping technique. Fig. 9 is the patient-specific tracheal stent (silicone) made by rapid prototyping technique through 3D printing in our lab. By this means, the personalized stent can perfectly fit into the trachea of each individual patient so that the hyperplasia of the granulation tissue may be suppressed and the incidence of tracheal restenosis may be reduced or even prevented, thus improving the patients' quality of life.

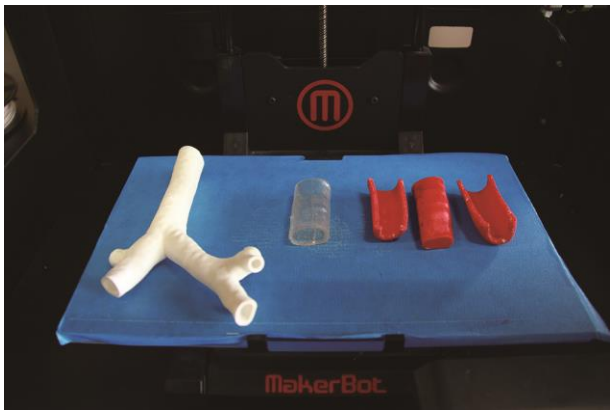

Figure 9: Patient-specific tracheal stent (silicone) made by rapid prototyping technique through 3D printing

Acknowledgments: We acknowledge the National Natural Science Foundation of China for supporting the project via the grant number 11472062, 11002034 and 11402037. We also acknowledge the finacial support from the Education Department of Jiangsu Province (No. 13KJB180001) and the technique support got from the ADINA Company in USA.

References

Chaure, J.; Serrano, C.; Fernández-Parra, R.; Pena, E.; Lostale, F. et al. (2016): On studying the interaction between different stent models and rabbit tracheal tissue: numerical, endoscopic and histological comparison. *Annals of Biomedical Engineering*, vol. 44, no. 2, pp. 368-381.

Desmoulière, A.; Redard, M.; Darby, I.; Gabbiani, G. (1995): Apoptosis mediates the decrease in cellularity during the transition between granulation tissue and scar. *American Journal of Pathology*, vol. 146, no. 1, pp. 56-66.

Fernandez-Bussy, S.; Akindipe, O.; Kulkarni, V.; Swafford, W.; Baz, M. et al. (2009): Clinical experience with a new removable tracheobronchial stent in the management of airway complications after lung transplantation. *Journal of Heart and Lung Transplantation*, vol. 28, no. 7, pp. 683-688.

Fung, Y. C. (1995): Stress, strain, growth and remodeling of living organisms. *Theoretical, Experimental and Numerical Contributions to the Mechanics of Fluids and Solids*, vol. 46, no. 1, pp. 469-482.

Gesierich, W.; Reichenberger, F.; Fertl, A.; Haeussinger, K.; Sroka, R. (2014): Endobronchial therapy with a thulium fiber laser (1940 nm). *Journal of Thoracic and Cardiovascular Surgery*, vol. 147, no. 6, pp. 1827-1832.

Ghosh, A.; Malaisrie, N.; Leahy, K. P.; Singhal, S.; Einhorn, E. et al. (2011): Cellular adaptive inflammation mediates airway granulation in a murine model of subglottic stenosis. *Otolaryngology-Head and Neck Surgery*, vol. 144, no. 6, pp. 927-933.

Grewe, P. H.; Müller, K. M.; Lindstaedt, M.; Germing, A.; Muller, A. et al. (2005): Reaction patterns of the tracheobronchial wall to implanted noncovered metal stents. *Chest*, vol. 128, no. 2, pp. 986-990.

Kampmann, C.; Wiethoff, C. M.; Huth, R. G.; Staatz, G.; Mengel, E. et al. (2017): Management of life-threatening tracheal stenosis and traheomalacia in patients with mucopolysaccharidoses. *Journal of Inherited Metabolic Disease Reports*, vol. 33, pp. 33-39.

Lee, Y. C.; Hung, M. H.; Liu, L. Y.; Chang, K. T.; Chou, T. Y. et al. (2011): The roles of transforming growth factor-β1 and vascular endothelial growth factor in the tracheal granulation formation. *Pulmonary Pharmacology & Therapeutics*, vol. 24, no. 1, pp. 23-31.

Matt, B. H.; Myer, C. M.; Harrison, C. J.; Reising, S. F.; Cotton, R. T. (1991): Tracheal granulation tissue. A study of bacteriology. *Archives of oOtolaryngology-Head & Neck Surgery*, vol. 117, no. 5, pp. 538-541.

Nashef, S. A. M.; Dromer, C.; Velly, J. F.; Labrousse, L.; Couraud, L. (1992): Expanding wire stents in bengin tracheobronchial disease: indications and complications. *Annals of Thoracic Surgery*, vol. 54, no. 5, pp. 937-940.

Pierce, G. F.; Tarpley, J.; Yanagihara, D.; Mustoe, G. M. (1992): Neovessel and matrix formation and cessation of repair. *American Journal of Pathology*, vol. 140, pp. 1375-1388.

Pokharel, R. P.; Maeda, K.; Yamamoto, T.; Noguchi, K.; Iwai, Y. et al. (1999): Expression of vascular endothelial growth factor in exuberant tracheal granulation tissue in children. *Journal of Pathology*, vol. 188, no. 1, pp. 82-86.

Shaikh, M.; Kichenadasse, G.; Choudhury, N. R.; Butler, R.; Garg, S. (2013): Non-vascular drug eluting stents as localized controlled drug delivery platform: Preclinical and clinical experience. *Journal of Controlled Release*, vol. 172, no. 1, pp. 105-117.

Simone, T. M.; Higgins, P. J. (2015): Higgins inhibition of SERPINE1 function attenuates wound closure in response to tissue injury: a role for PAI-1 in re-epithelialization and granulation tissue formation. *Journal of Developmental Biology*, vol. 3, no. 1, pp. 11-24.

Sussman, T.; Bathe, K. J. (2009): A model of incompressible isotropic hyperelastic material behavior using spline interpolations of tension-compression test data. *Communications Numerical Methods in Biomedical Engineering*, vol. 25, pp. 53-63.

Tomasek, J. J.; Gabbiani, G.; Hinz, B.; Chaponnier, C.; Brown, R. A. (2002): Myofibroblasts and mechano-regulation of connective tissue remodelling. *Nature Reviews Molecular Cell Biology*, vol. 3, no. 5, pp. 349-363.

Van De Water, L.; Varney, S.; Tomasek, J. J. (2013): Mechanoregulation of the myofibroblast in wound contraction, scarring, and fibrosis: opportunities for new therapeutic intervention. *Advances in Wound Care (New Rochelle)*, vol. 2, no. 4, pp. 122-141.

Xu, H.; Ma, J.; Wu, J.; Xu, S. (2016): The value of esophageal stenting for the treatment of benign tracheoesophageal fistulas: case report. *International Journal of Clinical and Experimental Medicine*, vol. 9, no. 1, pp. 385-390.

Xu, W. H.; Xu, H.; Zhang, G.; Hu, M. H.; Lou, F. Y. et al. (2016): Implantation of metallic stent under direct visualization of flexible bronchoscope without fluoroscopic guidance on orotracheal intubated patients. *Journal of Respiratory Research*, vol. 2, no. 3, pp. 75-78.

Yokoi, A.; Nakao, M.; Bitoh, Y.; Arai, H.; Oshima, Y. et al. (2014): Treatment of postoperative tracheal granulation tissue with inhaled budesonide in congenital tracheal stenosis. *Journal of Pediatric Surgery*, vol. 49, no. 2, pp. 293-295.

Zöllner, A. M.; Abilez, O. J.; Böl, M.; Kuhl, E. (2012): Stretching skeletal muscle: chronic muscle lengthening through sarcomerogenesis. *PLOS One*.